Journal of
*Marine Science and Engineering*

MDPI

*Review*

# A Review of the Hydroelastic Theoretical Models of Floating Porous Nets and Floaters for Offshore Aquaculture

**Sarat Chandra Mohapatra * and C. Guedes Soares**

Centre for Marine Technology and Ocean Engineering (CENTEC), Instituto Superior Técnico, Universidade de Lisboa, Av. Rovisco Pais, 1049-001 Lisboa, Portugal; c.guedes.soares@centec.tecnico.ulisboa.pt
* Correspondence: sarat.mohapatra@centec.tecnico.ulisboa.pt

**Abstract:** The present review focuses on the theoretical model developments made in floating flexible net fish cages and the floating bodies application to offshore aquaculture. A brief discussion of the essential mathematical equations related to various theoretical models of flexible net cages in the frequency domain is presented. The single and array of floating or submerged flexible net cages connected with or without mooring lines are discussed. Further, as the combined effect of the hydroelastic behaviour of floaters and the flexible behaviour of fish cages are necessary to assess their efficiency and survivability from structural damages, the issues and the knowledge gap between the recent and future models are also discussed. In conclusion, the practical suggestions concerning advancements in future research and directions within floating flexible net cages and the hydroelastic response of elastic floaters are highlighted.

**Keywords:** aquaculture; flexible net-type structure; offshore fish cages; analytical models; array of net cages; mooring lines



**Citation:** Mohapatra, S.C.; Guedes Soares, C. A Review of the Hydroelastic Theoretical Models of Floating Porous Nets and Floaters for Offshore Aquaculture. *J. Mar. Sci. Eng.* **2024**, *12*, 1699. https://doi.org/10.3390/jmse12101699

Academic Editors: Decheng Wan and Constantine Michailides

Received: 27 July 2024
Revised: 18 September 2024
Accepted: 19 September 2024
Published: 25 September 2024



## 1. Introduction

Researchers have been developing floating, flexible net cages for several years. These cages are designed to be cost-effective, environmentally friendly, reusable, and rapidly deployable. They are also highly reliable as wave absorbers, protecting marine structures from damage resulting from harsh maritime conditions. The past two decades have noticed a significant increase in the use of flexible net structures for fish farming due to the observed reduction in water turbulence within the cages [1–3], demonstrating that porous membranes can furnish a tranquillity area for fish farms [4].

Another interesting aspect of offshore aquaculture cages is the study of hydroelastic analysis of fish cages [5] concerning elastic floaters [6]. Hence, as offshore aquaculture farming is increasing exponentially, proper modelling of cages for different geometries to offer large-scale fish farms with multiple cages is essential to increase worldwide seafood production [7] by considering all environmental conditions, environmental depth, and hydrodynamics behaviour of cages. Importantly, when waves are scattered by the cages coupled with floaters, the hydroelastic response of elastic floaters is required to be analysed in detail as wave-floater interaction serves as a crucial component in the development of floating offshore fish farms.

From the aquaculture engineering perspective, the fish cage model associated with wave–elastic floater interactions may include varying vertical movements of floating structures, along with changes in acceleration, velocity, and wave overtopping and the hydroelastic effects of floaters of fish cages [8]. Due to environmental conditions, the deformation of circular elastic floaters can be significant as offshore fish cages relate to joints and mooring lines. The dynamic response and wave-induced forces, along with elastic floaters via hydroelasticity, are useful in designing the building and in fatigue analysis of offshore fish cage models for aquaculture. Therefore, the hydroelastic response via structural deformations of n-modes of oscillations in a single (Figure 1a) or an array of cages with elastic

floaters (Figure 1b) based on an analytical approach presents a difficult challenge because of the diffracted and scattered waves from other elastic floaters.

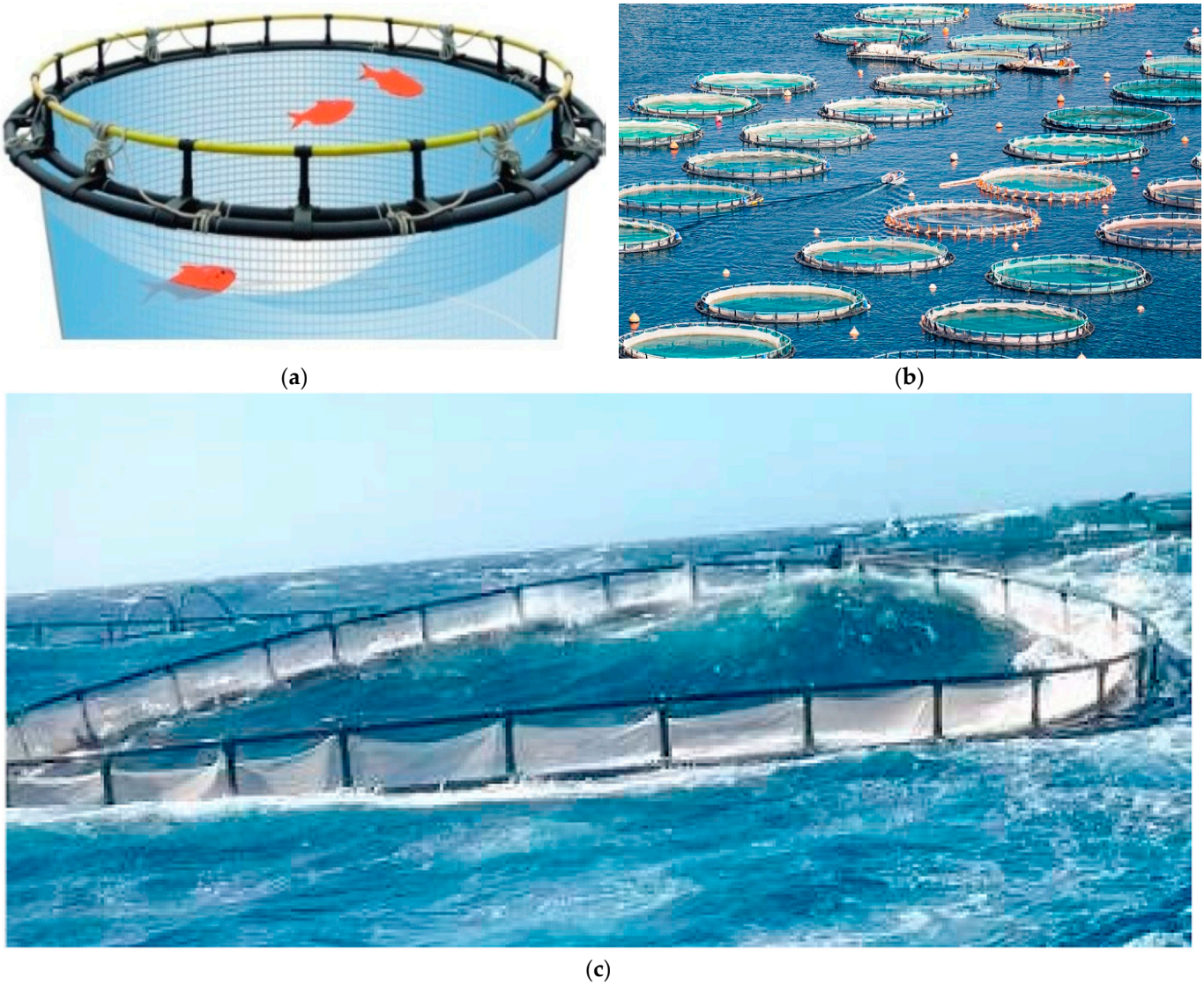

(**a**) (**b**)

(**c**)

**Figure 1.** (**a**) A schematic representation of an individual cage featuring a floater composed of double tori [8], (**b**) an array of cages set up in close proximity to one another [8], and (**c**) elastic circular floater deformation in a fish cage [6].

A review of the recent developments of various methodologies for the applications of flexible porous membranes (FPM) and fish cages was presented [4]. The review comprehensively analyzed fish cage designs, encompassing both conventional nearshore fish farms and the emerging new generation of offshore aquaculture facilities. It highlights the specific challenges that offshore fish farming faces, offering insights into the complexities of this emerging technology [9]. An analysis of the studies concerning net hydrodynamics was presented, focusing on the hydrodynamic loads, dynamic responses, and the flow-wave dynamics surrounding the nets, along with an exploration of unresolved research challenges and potential future avenues that are crucial for promoting sustainable aquaculture development [10]. A review of the construction and functionality of net cages by considering fish behaviour related to upcoming engineering advancements in the area of hydrodynamics for aquaculture cages was presented [11]. An analysis of the environmental elements linked to the intensification of aquaculture and their impact on aquatic ecosystems as well as past, present, and future aquaculture trends in coastal/offshore, land, and aquatic landscapes

were discussed [12]. An analysis of the advantages of farming in offshore aquaculture and compatibility with oceanography potential was presented in [13]. An examination of worldwide performance evaluation techniques and approaches for relocating fish farms to offshore locations, aimed at promoting a more sustainable growth of aquaculture, indicated that the fish pens will encounter more challenging environmental conditions [14].

The above literature confirms that to our best knowledge, no review has been reported, especially regarding the recent developments of theoretical models and the importance of the hydroelastic response of elastic floaters coupled with floating flexible fish cage models' application to offshore aquaculture.

This review summarizes the analytical modelling approaches of the dynamic and hydrodynamic behaviour of floating flexible net cages in both time and frequency domain analysis as outlined in Section 2. Section 3 provides an overview of the advancements in various analytical models and a discussion of their results along with limitations based on various theoretical methodologies. Section 4 presents the equation for the hydroelastic behavior of floaters within the scope of linear wave theory. Finally, Section 5 offers a concise overview of the conclusions and future perspectives of this review on the use of flexible porous net cages. associated with environmental conditions, depths, and mooring systems.

## 2. Modelling Approaches for Floating Fish Cage Systems Based on the Theoretical Formulations

The basic assumptions in terms of structural characteristics during flexible fish cages modelling based on analytical and numerical formulations are highlighted below.

Basically, in a dynamic analysis, the analytical modelling for net-type structures [15] draws upon subsequent assumptions.

(i) The FPM is represented as strings with consistent mass density that operate under uniform tension. The use of FPMs in fish cage modelling and breakwater applications is an excellent option due to their numerous advantages over rigid and nonporous structures. Their porosity aids in dissipating wave energy and is vital for understanding the dynamics of oscillatory flow, as it allows for the measurement of velocity, pressure fields, and wave heights within the porous structure. Dissipation phenomena serve a vital function in the transmission area, and the flexible porous structure acts as a filter, effectively removing larger frequencies as the oscillation moves toward the sheltered side of the structure [16]. Additionally, it has been observed that the water within the fish cages remains significantly calmer than the surrounding waters outside the fishnets, indicating that FPMs can create a tranquil zone ideal for fish farming. However, Ref. [17] indicated that modelling FPMs as strings or beams is an excessive simplification, and the proposed shell membrane theory can be used to address this oversimplification.

(ii) The analysis of waves moving past a porous membrane is designed according to Darcy's Law [4], and the constraints of applying Darcy's Law to the analysis of waves traversing a porous structure were discussed in [18].

(iii) The fluid is characterized as incompressible and inviscid, with irrotational motion, allowing for the presence of a velocity potential (VP) and the application of linear wave theory. Under the linear potential theory, the simplified geometries of porous rectangular, cylindrical, and hexagonal structures with limited environmental parameters are solved (for example [15]). Nonetheless, Ref. [19] highlighted that the predicted response of sloshing is expected to be infinite when applying linear potential flow theory in place of finite amplitude effects in practice. Further, the hydrodynamic drag on net structures depends on Reynolds number with respect to the twine diameter of the net. In the potential flow model, there is no dependence on Reynolds number.

(iv) It is presumed that both the amplitude of the incoming wave and the structural motions are small.

In the frequency domain, under linear wave theory, the frequently employed methods for the analysis of the dynamics of flexible porous structures are the MEFEM [20], the

BEM [21], the least square approximation method [15,20], the multipole expansion method (MPEM) [22], and Green's function technique (GFT) [23].

It may be noted that Darcy's Law posits that when flowing through a porous media, a fluid's velocity is proportional to the difference in pressure across the two sides of that structure. The constant of proportionality is a complex number, with its imaginary component associated with the inertia effect. This component can be disregarded when the porous structure is narrow and the holes are relatively small. The real component, known as the porous-effect parameter, indicates viscous effects and that can be directly from experimental data [24].

In general, Darcy's Law as it pertains to FPMs or net-type structures could be represented as shown in [4]

$$\vec{V} = -(k_0/\rho\omega)G\nabla p + (\partial\zeta/\partial t), \quad (1)$$

where $\vec{V}$ is the vector representing flow velocity, and G denotes the parameter for porous effects described as $G = G_r + iG_r = (\gamma/k_0 b) \times ((f + iS)/(f^2 + S^2))$, $S = (C_m(1-\gamma)/\gamma)$, $\gamma$ represents the porosity constant, characterized as the ratio of the porous surface area to the overall membrane area, $f$ denotes the resistance force coefficient, $S$ signifies the inertial force coefficient, $C_m$ refers to the added mass coefficient, the variable $\rho$ indicates the fluid's density, $\omega$ represents the angular frequency, $k_0$ refers to the incident wavenumber, $b$ stands for the porous medium thickness, $p$ denotes the fluid pressure, and $\zeta$ indicates the deflection of the FPSs. Additionally, $t$ represents the time, $\nabla$ = gradient operator, and $f$ and $S$ can be assessed, as outlined in [25]. Darcy's Law is based on the assumption that the porous medium remains stationary. However, if the porous medium is in motion, the effects of inertia must be considered, as mentioned in [26]. However, Darcy's Law is used to consider the flow past the porous net. More emphasis has been given to the quadratic pressure drop condition for flow past porous structures, as discussed in [27,28].

An important aspect of modelling floating flexible fish cages coupled with elastic floaters is the designing of floating elastic floaters of different geometrics. Usually, in the analytical approach, the net-type structures (modelled as porous membrane based on Darcy's Law) are used for the dynamic analysis and wave-induced loads on fish cages under environmental conditions [15,29]. Meanwhile, the elastic floaters can be modelled using the Euler–Bernoulli beam theory for hydroelastic response, which may help model elastic floaters coupled with a floating flexible fish cage.

## 3. Dynamics of Floating Flexible Fish Cages under Analytical Approaches

The MEFEM is typically employed as the theoretical method for wave structure interaction problems in 2D [30] or in 3D [31]. The key concept of this approach is to first expand the VPs with suitable eigenfunctions and unspecified coefficients. The complex wavenumbers are determined by the solution of the related complex dispersion relation.

It may be mentioned that complex wavenumbers are associated with the complex dispersion relation (obtained from the third-order porous membrane-covered BC). The complex dispersion relation (2) possesses a limitless quantity of complex roots, among which, two are identified as wavenumbers $p_n$, $n = 0, I$ corresponds to the most progressive waves. Meanwhile, the two complex roots $p_n$, $n = II, III$ of the specific type $a \pm ib$ ($a$ = real part, $b$ = imaginary part) are identified as wavenumbers linked to the non-propagating wave modes, and the countless complex roots $p_n$, $n = 1, 2, 3 \ldots$, that are near the imaginary axis are classified as the evanescent wave modes.

$$\left\{(T_f p_n^2 - m_s)ik_0 G - K\right\}(p_n \tanh p_n H - K)\cosh p_n H - p_n(T_f p_n^2 - m_s)\sinh p_n(H-h)(p_n \tanh p_n h - K)\cosh p_n h = 0 \quad (2)$$

where $G$ represents the parameter for the porous effect, and other symbols can be found in [15].

Subsequently, the unknown constants are established by applying different BCs with appropriate orthogonal properties or the LSAM to obtain a matrix system.

The impact of a vertical fishnet on the interaction of a surface wave was analyzed in FWD [20] and solved by employing the MEFEM and the LSAM. They found that in general, (i) the hydrodynamic force rises as stiffness increases, (ii) a more flexible barrier deforms with respect to the force and for large values of stiffness, the hydrodynamic pressure decreases with depth, and (iii) the pressure force demonstrates a type of 'instability' at a specific stiffness value, shifting from up to down mode when the threshold is reached. The physical mechanism behind the instability is the variation of the sign of the pressure gradient that results in wave energy dispensation caused by the limited reflection from the fishnet, and it depends on the quantity of energy dissipated by the barrier. The hydroelastic analysis was conducted for surface wave interaction using concentric systems of porous and flexible cylinders, where the inner cylinder remains rigid while the outer cylinder is both porous and flexible [32]. The scattering potentials were evaluated using the FBEM and LSAM. They discovered that the deflection was greatest near the free surface and was more significant for the surface-piercing system than the bottom-touching cylinder system with identical drafts. In contrast, the floating flexible cage exhibited the greatest deflection just above the mid-point of the cylinder, closer to the upper surface.

GFT has been used to analyze the dynamics of FPMs on the hydroelastic behaviour of floating beams based on the elastic beam theory. GFT and Green's identity were adopted to determine numerical solutions. A few researchers analysed a couple of problems associated with wave scattering by floating and submerged bodies of floating rectangular elastic plate or porous structures based on GFT. Nonetheless, the use of the GFT with floating flexible fish cages has yet to be investigated.

There are very few mathematical formulations associated with the floating flexible fish cage model-based linear water wave theory available in the literature, which is detailed as follows. A linear mathematical formulation was developed for a freely floating flexible two-dimensional closed fish cage in order to examine the sway, heave, and roll motions induced by waves in [33] (Figure 2). They noted that the absence of tension might result in snap loads on the material, which could lead to fatigue. They examined a compact, flexible fish cage compared to the larger aquaculture net cages currently utilised in Norway. It was seen that the closed flexible fish cage exhibits flexibility and operates hydro-elastically, and its response is significantly influenced by both its geometry and the level of the filling.

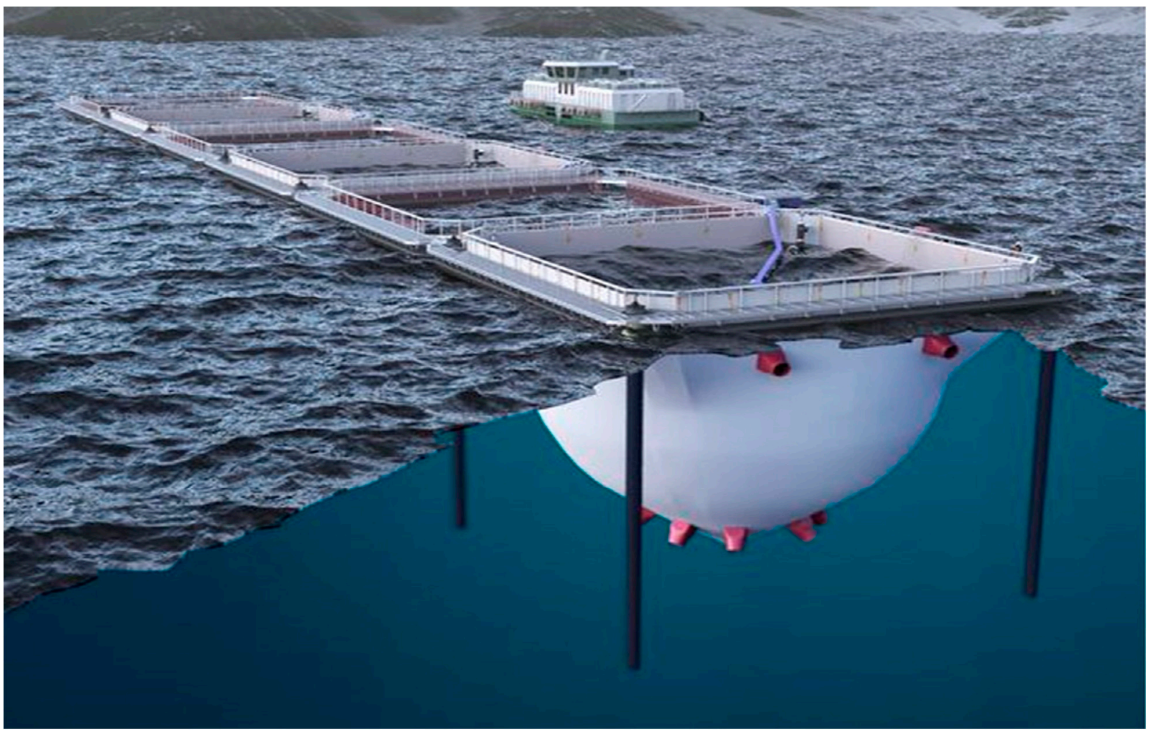

**Figure 2.** Closed flexible fish cage [33].

Figure 3, consisting of a vertical cylindrical flexible net cage (modelled as a one-dimensional string) and a permeable base, is typically used for farming sea fish [34]. They solved analytically by applying the FBEM and LSAM under the linear water wave theory. An analytical model of a concentric cylindrical cage was presented based on Darcy's Law and under linearized potential flow theory [35]. Their findings indicated that porosity decreases the forces acting within the cage system by absorbing the utmost amount of wave energy. Additionally, they observed that membrane deflection diminishes as the porous effect parameter value increases, and as the radius of the cage increases, the vertical deflection of the membrane rises. However, the work carried out [35] did not consider mooring lines to prevent structural damage from strong waves and currents during storms, nor did it consider the impact of wave trapping caused by opposing currents.

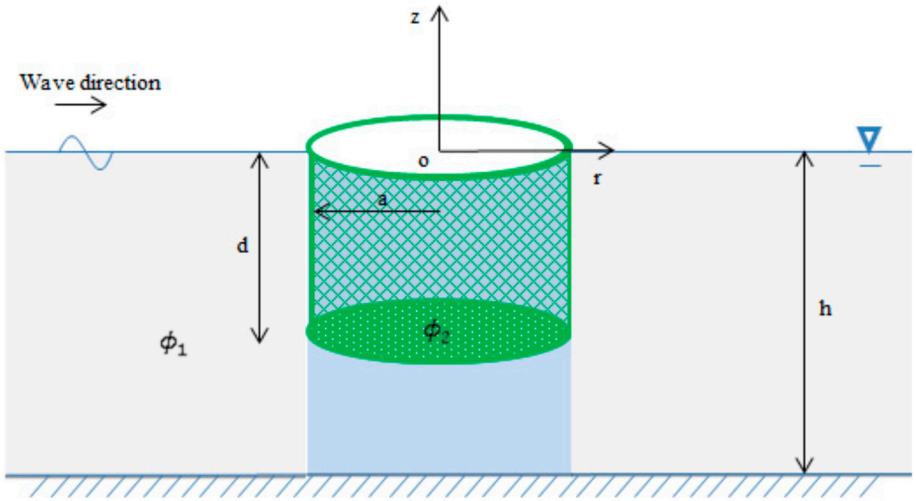


**Figure 3.** Flexible circular cage system [34].

Wave interaction with a floating porous circular cylinder was analysed based on the potential flow theory by employing the MEFEM [36]. The analytical solution was validated against independent experimental test results. They discovered that the wave-radiating damping includes a second term that accounts for the effects of porosity $\sigma$ as incorporated in Equation (3). In this model [36], the effects of environmental conditions, such as varying water depths and following or opposite current loads, were not taken into account, and there were no edge conditions imposed (for example, to avoid structure failure in storm waves and currents during typhoon events, any kind of moored edge conditions at the structural boundaries), which limits its applicability in practical engineering case studies.

$$\mu_{ij} = \frac{2\omega C_0}{\pi}\rho \int_0^{2\pi} A_i(\theta)A_j^*(\theta)d\theta + \omega\sigma\rho \,\mathrm{Re}\left((\varphi_i^{(out)} - \varphi_i^{(in)}) \times (\varphi_i^{(out)*} - \varphi_i^{(in)*})ds\right). \quad (3)$$

As per the slender body theory, a semi-analytical approach was presented, and matched asymptotic expansions were utilized to ascertain the vertical accelerations of a series of partially submerged elastic circular floaters subjected to regular waves in [8] and compared with experiments in [6]. The obtained analytical solution was compared with model tests, and they found that as the wavenumber rises, the floater hydro-elastic interaction becomes important. As the wavenumber rises, the accelerations of the middle torus increase at a slower rate compared to the single torus in the waves. This phenomenon occurs because, as the wavenumber increases, the portion of the wave reflected by the upper torus and the transmitted wave reaching the middle torus diminishes. In addition, as was highlighted in [15], horizontal accelerations play a crucial role in both engineering design and operations for offshore aquaculture floating flexible net cages. In addition, upstream, the floaters exhibit more pronounced vertical movements compared to a single

floater in wave conditions. Also, they compared their model with ANSYS Aqwa 2019 software in sea waves that were limited to rigid tori.

Circular cages are organized in mooring grids in single, double, or triple rows, with shared spacing in between them, typically chosen as a multiple of the radius of their circular floaters (refer to Figure 4). Figure 5 illustrates the comparison of non-dimensional wave amplitude $\zeta_a/\zeta_0$ ($\zeta_0$ is incident wave amplitude) from the current method [6] and ANSYS Aqwa, regarding the scattered wave amplitude at the front ($\beta = \pi$) and back ($\beta = 0$) of a semi-submerged circular rigid floater with a/c = 0.024, plotted against dimensionless radial distance ($\rho/c$). It has been noted that as $\rho/c$ rises, the accuracy of [6] improves, and this method has effectively determined both the maximum and minimum locations and the corresponding wave heights.

**Figure 4.** An array of cages installed nearby within an aquaculture farm [6].

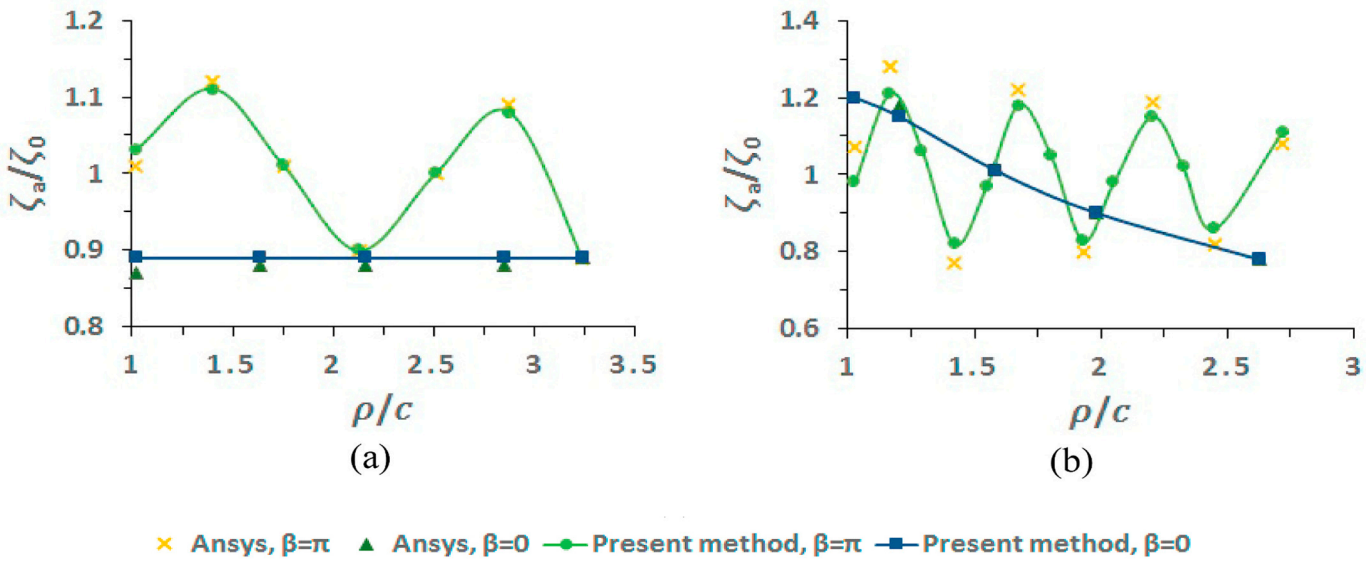


**Figure 5.** Comparison of the current theoretical model and ANSYS AQWA for vertical acceleration of semi-submerged torus with (**a**) $\vartheta a = 0.05$, (**b**) $\vartheta a = 0.15$ [6].

An analytical wave interaction model of a anchored floating flexible cage was presented in [15] to analyze the wave-induced forces on the net cage.

The BCs and governing motion of the cage surface on $r = a, -h \leq z \leq -d$ are given as

$$\phi_{1r} = \phi_{2r} = ik_0 G(\phi_2 - \phi_1) + i\omega\eta cos\theta, \tag{4}$$

$$d_z^2\eta + (m_m\omega^2/T)\eta = (2ai\omega\rho/T)\int_0^{\pi}(\phi_2 - \phi_1)\cos(\pi - \theta)d\theta, \tag{5}$$

where $\eta$ is the deflection of the cylinder, $r$ represents the radial distance measured from the $z$-axis, $\phi_1$ = VP in region 1, $\phi_2$ = VP in region 2, $G$ =porous effect parameter, $k_0$ = wavenumber, $d$ = gap height, $T$ = membrane tension, $h$ = water depth, and $\theta$ is the angle with horizontal axis in the 3D polar coordinate system ($r$, $\theta$, $z$).

The bottom or base of the cylindrical net cage is fitted with a horizontal porous surface and is often considered a two-dimensional horizontal membrane or rigid porous plate [34], and the BCs are as follows (as in Equations (4) and (5)):

$$\phi_{2z}|_{z=-d\pm 0} = ik_0 G\left(\phi_2|_{z=-d-0} - \phi_2|_{z=-d+0}\right) - i\omega\xi \text{ on } r < a,\ z = -d, \tag{6}$$

$$\left(\nabla_{r\theta}^2 + \frac{m_m\omega^2}{T}\right)\xi = \left(-\frac{i\rho\omega}{T}\right)\left(\phi_2|_{z=-d-0} - \phi_2|_{z=-d+0}\right) \text{ on } r < a,\ z = -d, \tag{7}$$

with $\xi$ = deflection net, and $\nabla_{r\theta}^2$ is the Laplacian or Laplace operator.

As per the potential flow theory, applying suitable BCs in the water region and the structural BC along with the continuity condition, the wave-net interaction problem can be solved. The model of surface wave scattering caused by a vertically positioned, flexible fishnet in FWD was resolved by the MEFEM and the LSAM [15]. Figure 6 demonstrates that as the net stiffness increases, the net's deformation decreases, thus increasing the reflection coefficient. Additionally, the comparison of displacement between the simulations of the theoretical and numerical model shows a strong agreement (Figure 6).

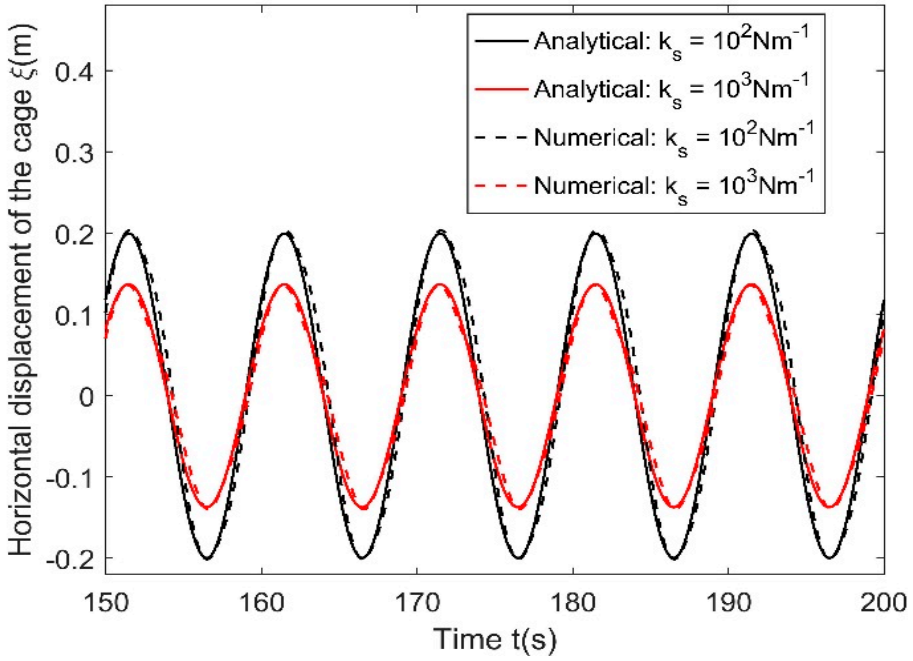


**Figure 6.** Comparison results of horizontal displacements [15].

Further, the model developed [15] was extended under the action of current loads on the floating flexible fish cage with $h_2 = 50$ m, $h_1 = 7$ m, $a = 5$ m by comparing with the FEM analysis [29] in Figure 7. It studied the net cage's dynamic response by examining various results on horizontal wave loads and axial forces acting on the mooring lines for

different structural and physical parameters. In the mathematical formulation [29], the opposite current was not considered, which meant that the numerical analysis could not conduct a wave-trapping assessment in conjunction with the prevailing current.

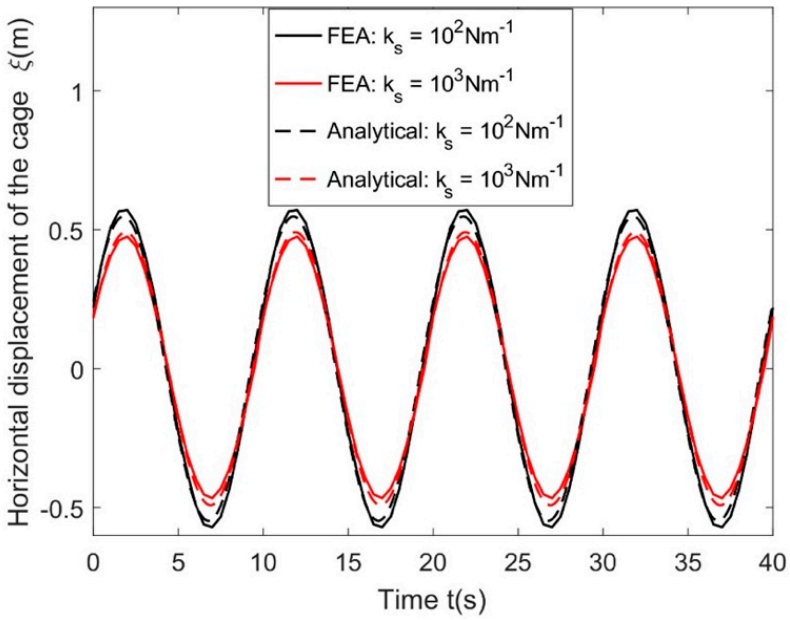


**Figure 7.** Comparison: cage horizontal displacement for different mooring stiffnesses $k_s$ [29].

The condition in terms of the pressure differences between the boundary $G_p$ and inside the cage ($R_2$) (see Figure 8) is given by

$$\left(-T\nabla_{r\theta}^2 + m_m\frac{\partial^2}{\partial t^2}\right)\xi = -(P_3(r,\theta,z,t) - P_2(r,\theta,z,t)) \tag{8}$$

where $P_j(r,\theta,z,t)$, is the linearized hydrodynamic pressure in the jth region and is given by

$$P_j(r,\theta,z,t)) = -\rho\left(\frac{\partial\Phi_j}{\partial t} - gz\right), \text{ for } j = 2,\ 3,\ z = -h \tag{9}$$

with the symbols used in Equations (8) and (9) being the same as in Equation (7).

The examination of the 3D displacements of the cage at various current speeds indicates that the cylindrical cage exhibited greater stability (occurs due to the smaller deflection and lower horizontal force acting on the cage) at smaller current speeds [29]. Under the action of current, the condition for the linearized free surface is expressed as [29]

$$(\partial_t + u_1\partial_x + u_2\partial_y)^2\Phi_j + g\Phi_{jz} = 0 \text{ for } j = 1,2\ ,\ z = 0. \tag{10}$$

The kinematic BC with uniform current yields

$$\Phi_{2z} = \Phi_{3z} = \eta_t + u_1\partial_x + u_2\partial_y + ik_0G(\Phi_3 - \Phi_2) \text{ at. } z = -h_1 \tag{11}$$

where $u_1$ refers to current velocity along $x$-direction, $\eta_t$ = partial derivative of cage deflection, and $u_2$ = current speed along $y$-direction.

Additionally, the membrane deflection $\xi(z,t)$ satisfies the linearized dynamic condition:

$$\left(m_m\frac{d^2}{dt^2} - T_g\frac{d^2}{dz^2}\right)\xi = 2a\rho\int_0^\pi\left(\frac{\partial\Phi_2}{\partial t} - \frac{\partial\Phi_1}{\partial t}\right)\cos(\pi-\theta)d\theta, \tag{12}$$

In this context, $T_g$ represents the consistent tensile force exerted on the cage, while $m_m$ denotes the mass of the membrane, and $\phi_1$ and $\phi_2$ refer to the VP for the outer and inner regions (see Figure 8).

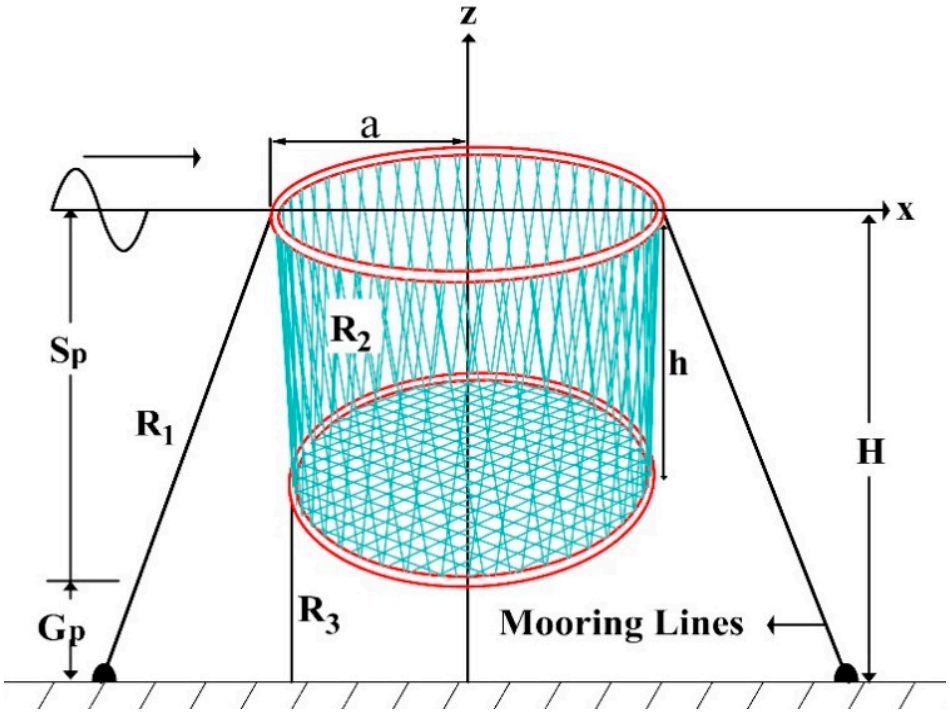


**Figure 8.** Schematic representation of a moored floating flexible net cage [15].

The conditions in terms of the continuity of velocity and pressure at the interface $r = a$ along the gap are read as

$$\frac{\partial \Phi_1}{\partial r} = \frac{\partial \Phi_3}{\partial r} \text{ at } r = a, z \in G_p \tag{13}$$

$$\Phi_1 = \Phi_3 \text{ at } r = a, z \in G_p \tag{14}$$

A semi-analytical single gravity-type cylindrical open fish cage in which the cage net is designed as a FPM and the hydroelastic characteristics of the net cages along with structural deflection and wave loading on the cages are analyzed [5] (see Figure 9). They observed the following: (i) as the porosity of the fish net rises, the amplitude of transverse deflection at the top section of the net chamber lessens, while the value at the bottom section shows a little increase because of the considerable obstruction affecting the flow near the wave surface; (ii) the axial tension in the cage greatly influences the porous effect of the fishnet; (iii) as per [37], in theory, the parameter representing the porous effect is expected to approach ∞ when the net interface becomes fully permeable. However, the equation for the porous-effect parameter does not conform to this scenario, leading to the conclusion that a more appropriate formula for the porous parameter is necessary for future research.

The dynamic responses of an array of submerged flexible fish cages were analyzed based on a semi-analytical solution under the linear wave theory, where the net cages were modelled as a porous cylindrical shell [38]. They observed that increasing the wavenumbers, cage spacing, and overall porosity are advantageous for reducing the interference impacts of waves in a cage arrangement.

Figure 10 illustrates the 3D shapes of the net chamber, depicting the maximum deformation at various submerged depths, with deflection values increased by a scale factor of five. A minimal wave response of the cage is noted when it is submerged at $d_1/h$.

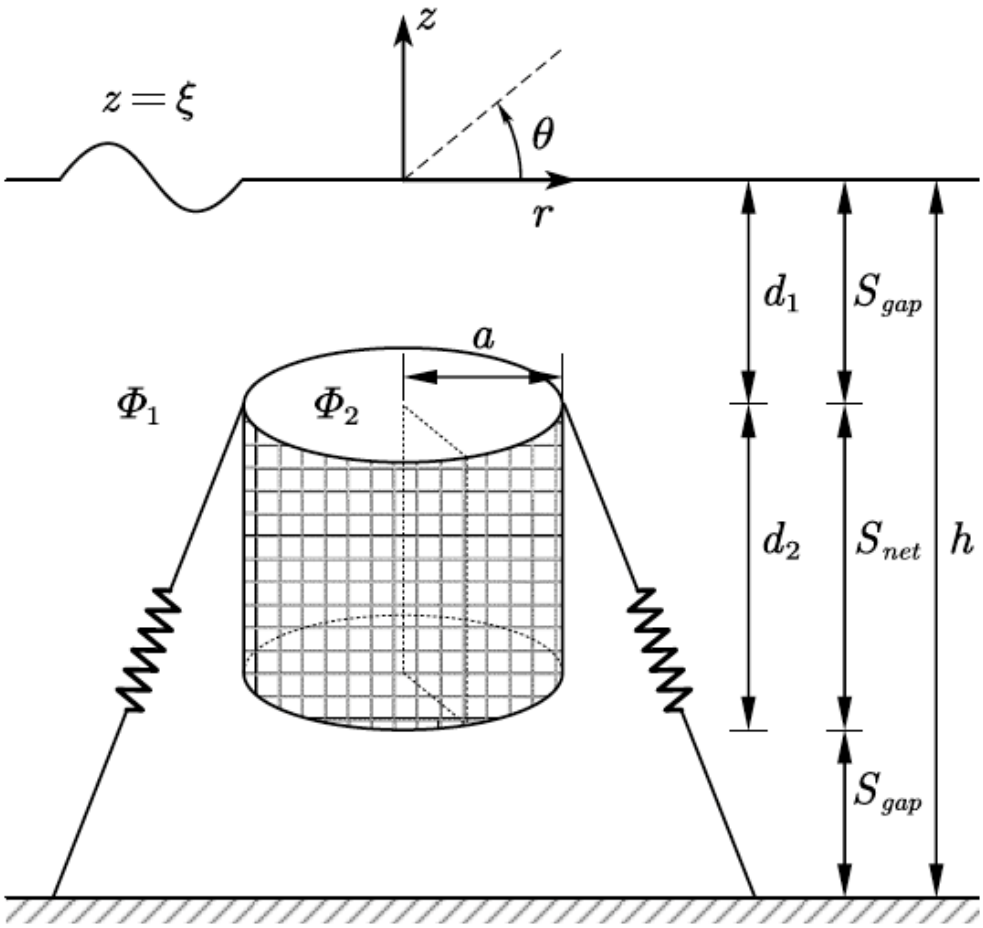


**Figure 9.** Submerged flexible fish cage [5].

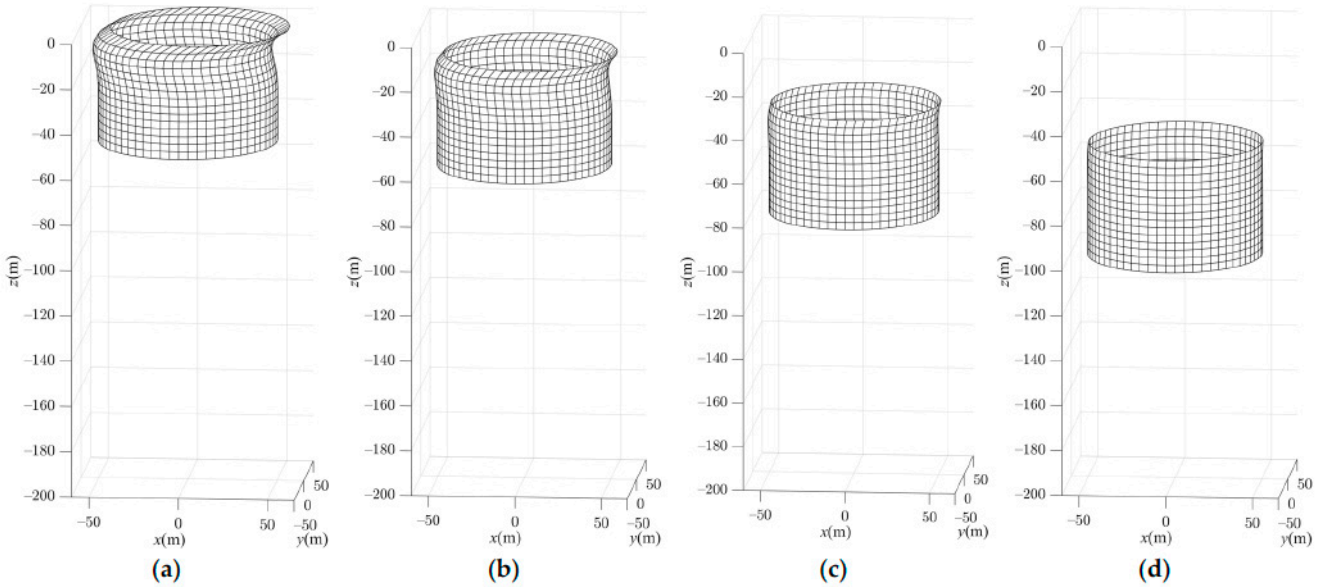


**Figure 10.** 3D deformation of a cage at various submerged depths [5]: (**a**) $d_1/h = 0$, (**b**) $d_1/h = 0.05$, (**c**) $d_1/h = 0.15$, (**d**) $d_1/h = 0.25$.

The hydrodynamic forces and structural reactions of two free-floating flexible circular cylinders subjected to surface waves were assessed using an approximate method devel-

oped by [39]. It was noted that different wave and structural parameters have a substantial impact on the hydrodynamics and dynamic behavior of individual cylinders.

The forces generated by wave excitation on a series of floating circular porous cylinders are analyzed applying the MEFEM within the framework of the diffraction potential theory, as described by [40]. It was indicated that the porosity of the circular cylinders is highly effective in significantly decreasing both wave excitation forces and wave run-up.

Recently, an array of floating flexible cylindrical fish cages in wave-current loads based on a theoretical study was developed [41] (see Figure 11). They analyzed the flow field over the cages, deflections, and wave forces on the cages for various structural and physical characteristics. With the increase in mooring stiffness and current velocities, the wave loads and cage displacements also rise, which is attributable to the stronger hydrodynamic forces generated by the more intense currents. In this case, the authors did not consider elastic floaters to study the effect of current combined with flexible net cages.

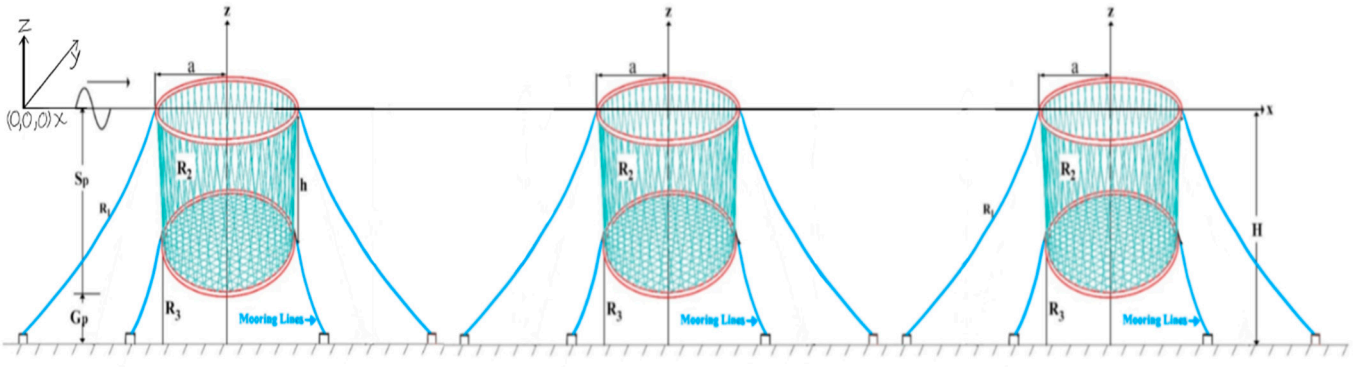


**Figure 11.** Moored floating flexible net cages [41].

In Figure 12, the comparison shows that the amplitude of horizontal displacement for a triple cage is significantly less than that of both dual and single cages.

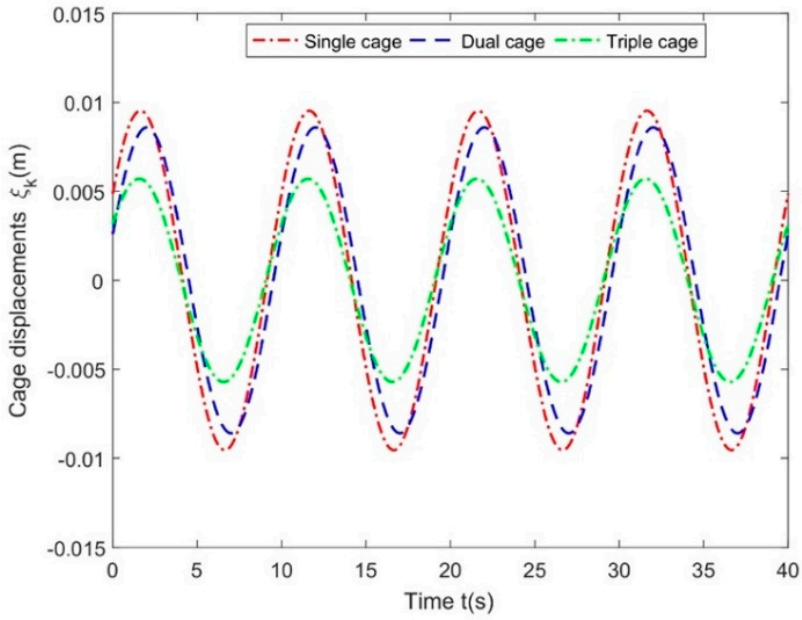


**Figure 12.** Comparison of deflections versus time t(s) [41].

On the other hand, the analysis of wave diffraction caused by a bottom-standing cylinder with a random cross-section under linear waves was conducted [42], and an array of truncated cylinders [43] was analyzed using an analytical method. These two references could aid in examining the hydroelastic behavior of floating cylinders using the same methodology in future studies.

An analytical formula for the drag coefficients related to both normal and tangential forces in cylindrical fish cages (Figure 13) to study the effect of net solidity, mesh pattern, and flow directions was derived in [44]. Further, the derived theoretical drag force results were compared against experimental model tests for different parameters (Figure 14). It was observed that they agreed well with all three solidity ratios where the drag coefficients on flat net panels were measured to estimate both the normal and tangential forces on the fishing net meshes to identify the empirical constants within the theoretical equations. Additionally, the drag coefficients for normal and tangential forces proposed in [44] are applicable solely to nets exposed to steady and uniform far-field currents.

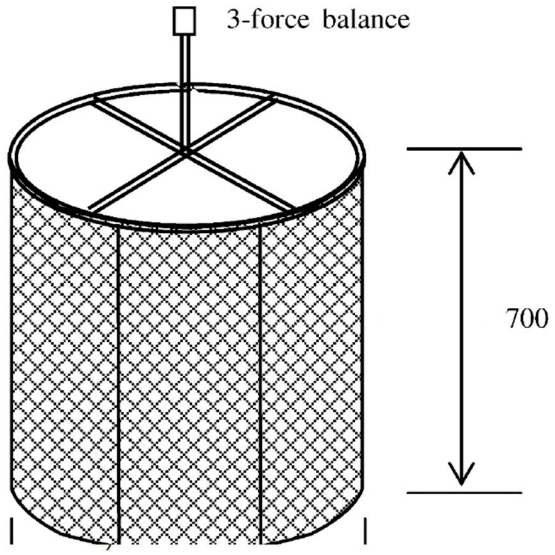


**Figure 13.** Schematic diagram of the cylindrical fish cage (adopted from [44]).

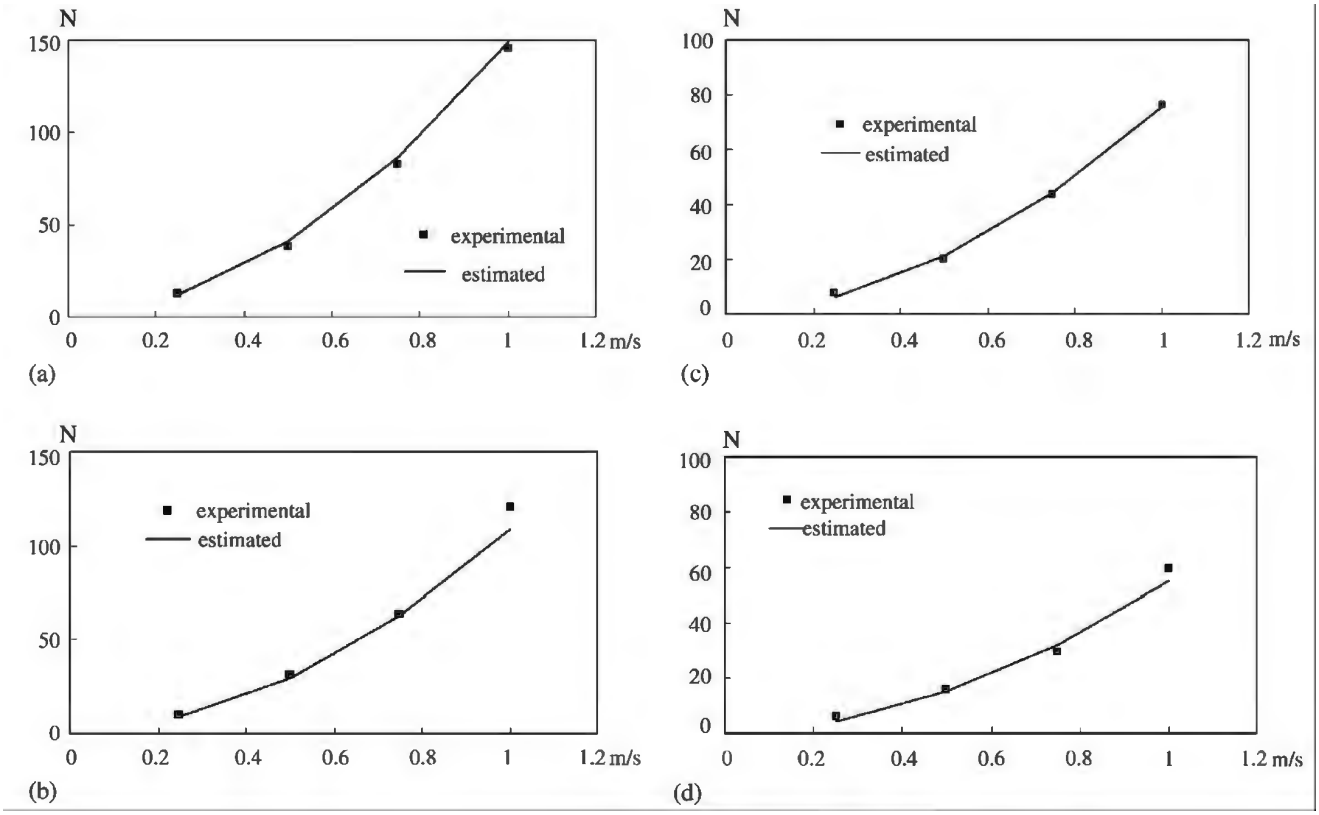


**Figure 14.** Comparison of drag forces between theoretical and experimental are plotted: (**a**) $\theta = 0^o$, $s = 0.223$; (**b**) $\theta = 30^o$, $s = 0.223$; (**c**) $\theta = 0^o$, $s = 0.128$; (**d**) $\theta = 30^o$, $s = 0.128$ [44].

The interaction between the linear waves and a submerged porous sphere applying the MPEM was studied semi-analytically, and an analysis was conducted regarding the hydrodynamic coefficients and wave-induced forces (wave strength) within the sphere [45] (Aquapod fish cage, see Figure 15). The cage was modelled based on Darcy's Law under the potential flow theory. They observed that the porosity parameter leads to a reduction in wave forces and added mass, while the damping coefficient experiences a notable increase across the range of wavenumbers (referring to deep water approximation solution as $kh \gg 1$, where $k$ is the wavenumber and $h$ is the water depth) (Figure 16). The results of the study [45] may be helpful in better understanding and analyzing the behavior of submerged spherical aquaculture cages.

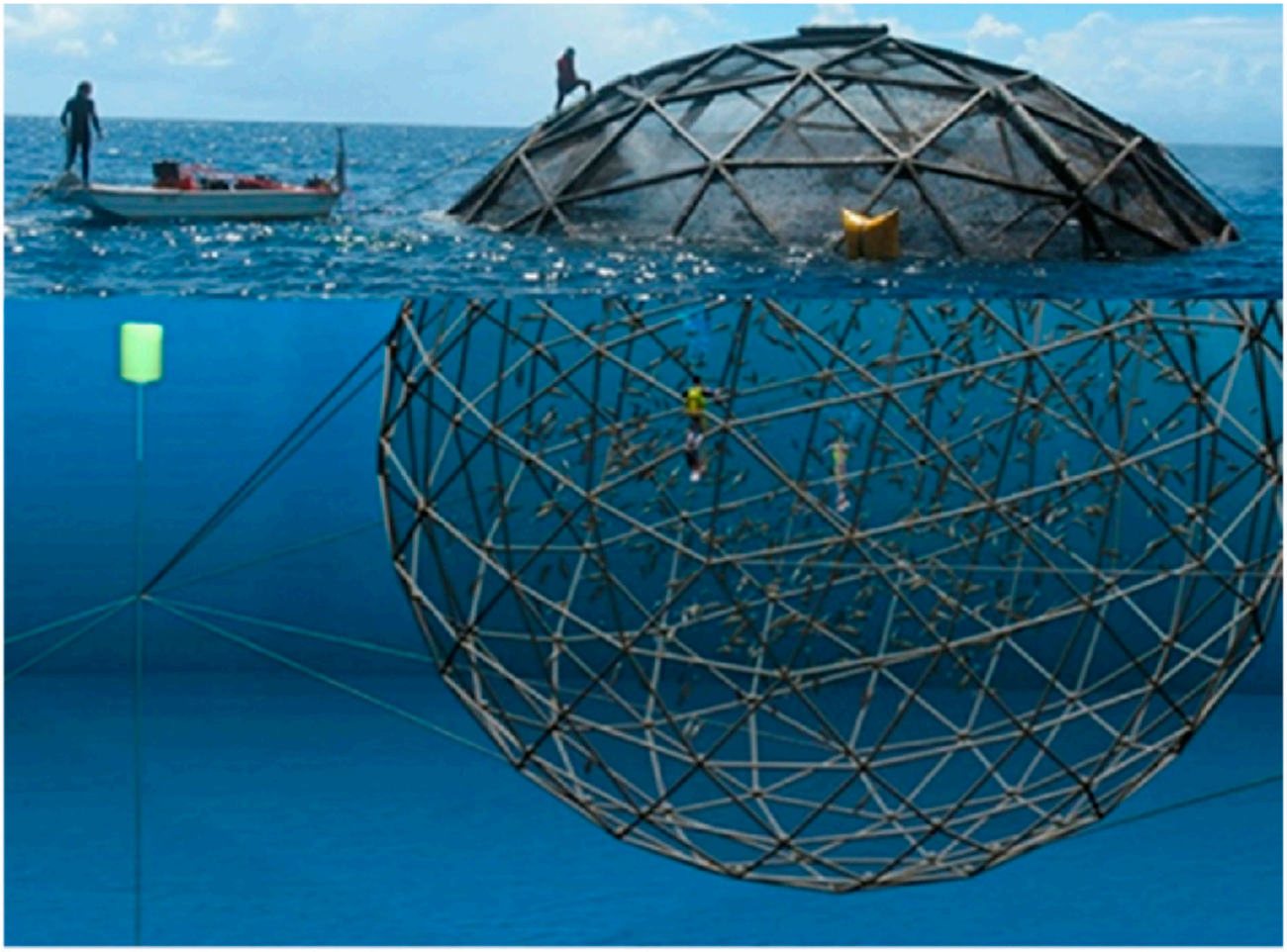

**Figure 15.** A cage for fish shaped like a sphere, (https://www.innovasea.com) [45].

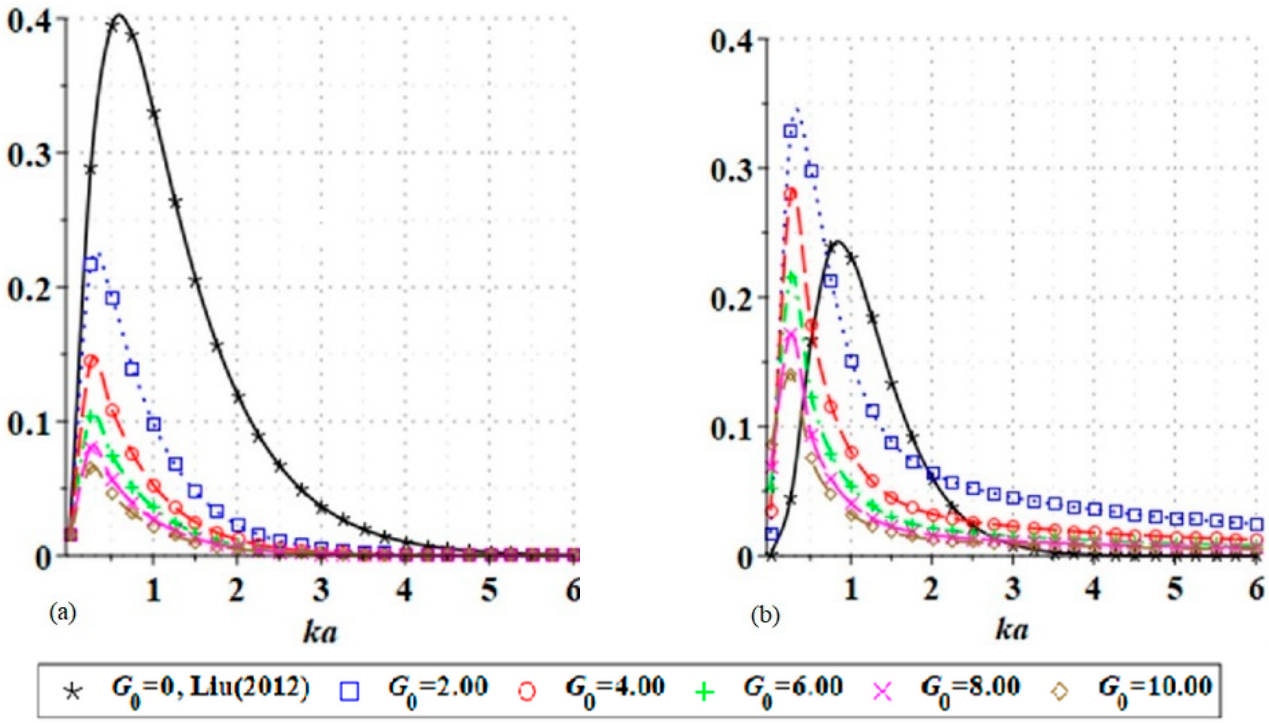


**Figure 16.** Hydrodynamic coefficients under varying porosity parameters $G_0$, $a$ = 1.0 m, and $z_0 = 1.5a$: (**a**) heave exciting force; (**b**) heave damping [45].

## 4. Linearized Theoretical Background for Hydroelastic Response of Elastic Floaters

Hydroelasticity plays a crucial role in assessing wave loads on floaters constructed from High Density Polyethylene (HDPE). Hydroelasticity is the interaction among inertial, hydrodynamic, and elastic forces [46]. Here, we analyze several earlier studies related to the hydroelastic behavior of floaters. A theoretical method was proposed to investigate the elastic deformations of the circular ring due to the influence of second-order waves, employing the curved beam theory [47]. An analysis on the combined influences of hydroelasticity and Morison's equation by exploring wave-induced forces was discussed in [48]. A slender-body theory has been formulated to analyze the low-frequency wave-induced responses of an elastic semi-submerged torus [49].

It is considered that a beam features a curvature in a plane with a radius $(r)$ and deforms by $\zeta$ in the vertical $y$-direction (see Figure 17). A coordinate system was established that features a curvilinear coordinate and radial coordinate $r$ along the beam that starts from the center of curvature in the absence of beam deformation. A segment of the beam with a small length $dx$ is examined (refer to Figure 18), and the figure illustrates the internal forces and moments that are acting on this portion of the beam. These include the bending moment $M_p$ around the $p$-axis, the torsional moment $M_q$ along the $x$-axis, and the vertical shear force $f_s$ directed along the $z$-axis.

An incident of regular waves interacting with a circular floater in FWD of infinite extended length is assumed. The elastic floater is formulated as the cartesian, and cylindrical coordinate system denoted as $(x, y, z)$ and $(r, \theta, z)$ with mean free surface at $y = 0$. On the other hand, the curved beam equation is represented by the Euler–Bernoulli beam theory with axial stiffness. The $y$-axis aligns with the axis of the torus and extends in the +ve- downward direction, and this refers to the radius of the central circular curve of the torus. The VP $\Phi(x, y, z, t) = \mathrm{Re}\{\phi(x, y, z)e^{-i\omega t}\}$ where Re is the real part and $\phi$ denotes the spatial complex VP that satisfies

$$\nabla^2_{xyz}\Phi = 0 \text{ in the fluid domain.} \quad (15)$$

where $\nabla^2$ denotes the Laplacian operator.

By considering minimal wave steepness and minimal vertical movements of the body in relation to the wave amplitude, the linearized kinematic and dynamic conditions on $y = 0$ are

$$\eta_t = \Phi_y, \tag{16}$$

$$\Phi_t + g\eta = 0. \tag{17}$$

By combining Equations (16) and (17), the linear form of the free surface BC can be obtained as

$$\partial_t^2 \Phi + g\Phi_y = 0, \text{ on } y = 0, \tag{18}$$

where the subscripts '$t$' and '$y$' denote the partial derivatives with respect to t and $y$, respectively.

The BC on the wetted body surface is given by

$$\frac{\partial \phi}{\partial n} = v.\vec{n} \text{ on } S_B, \tag{19}$$

where $v$ represents the velocity of the body with $\vec{n} = (n_1, n_2, n_3)$.

The Euler–Bernoulli beam equation satisfies the vertical motion $\zeta$ as

$$\left\{ EI\partial_x^4 - \partial_x(Q_{ax}\partial_x) + (EI/r^2)\partial_x^2 + m\partial_t^2 + 2a\rho g \right\}\zeta = N_1 + N_2 + N_3, \tag{20}$$

where the second term in Equation (20) denotes the bending stiffness, $EI$ = flexural rigidity of the torus, $\zeta$ = vertical motion of the torus, $r$ = the radius of the torus, $Q_{ax}$ = axial stiffness, $2a\rho g\zeta$ is generated through the alteration of the buoyant force caused by motion $\zeta$, $N_1(x)$ = vertical added mass and damping force, $N_2(x)$ = vertical wave excitation force, $N_3$ = vertical forces of the mooring line components, m is the torus mass, and $a$ = radius of cross-section of torus.

The response is symmetrical for waves moving in the +ve $x$, and the vertical motion $\zeta$ of the torus is expanded as

$$\zeta = b_0(t) + \sum_{n=1}^{\infty} b_n(t)\cos(n\alpha), \tag{21}$$

where $n$'s denote the elastic modes and their mode shapes stated as $x = \cos(n\alpha)$. $b_0$ and $b_1 \cos\alpha$ describes heaving at the axis of the torus and the vertical movement resulting from the pitch motion, respectively. Further, $x = r\cos(\alpha)$ and $y = r\sin(\alpha)$ are the coordinates of the torus centerline.

It may be noted that the hydroelastic response of the circular collar or floater is obtained by substituting values of $\zeta$ into Equation (20), and then Equation (20) is multiplied by $cosm\alpha$, $m$ = 0, 1, 2, ... and integrated over $\alpha = 0$ to $\pi$, which results in the right side of Equation (20). The motion equation for the amplitude of each mode $b_n(t)$ is then established. The MEFEM is applied to solve the BVP by studying radiation problems. In practice, the consistent interaction of waves with elastic floaters in severe weather conditions is not an ideal approach for conducting a hydroelastic analysis of these floaters. Consequently, taking into account nonlinear interactions provides a vital analysis of the displacement, deflection, and deformation of elastic floaters. Relative vertical movements between the floater and the sinker tube can result in snap loads within the netting, potentially leading to net rupture [50]. The impact of a well boat on a fish farm was examined, revealing that in severe weather conditions, the bending stress experienced by the floater could surpass the yield stress at both the interface between the well boat and the floater as well as at the points where the mooring lines connect to the floater [51].

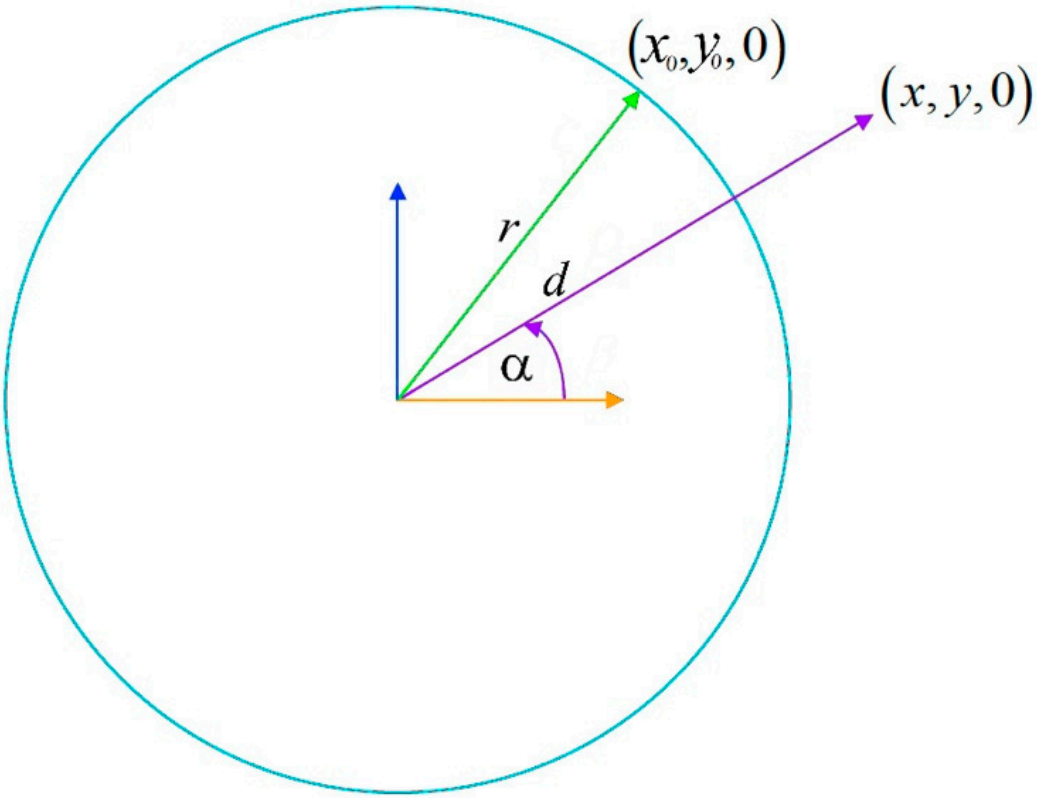


**Figure 17.** Plane view of a circular elastic floater (modeled as beam) with coordinate definition.

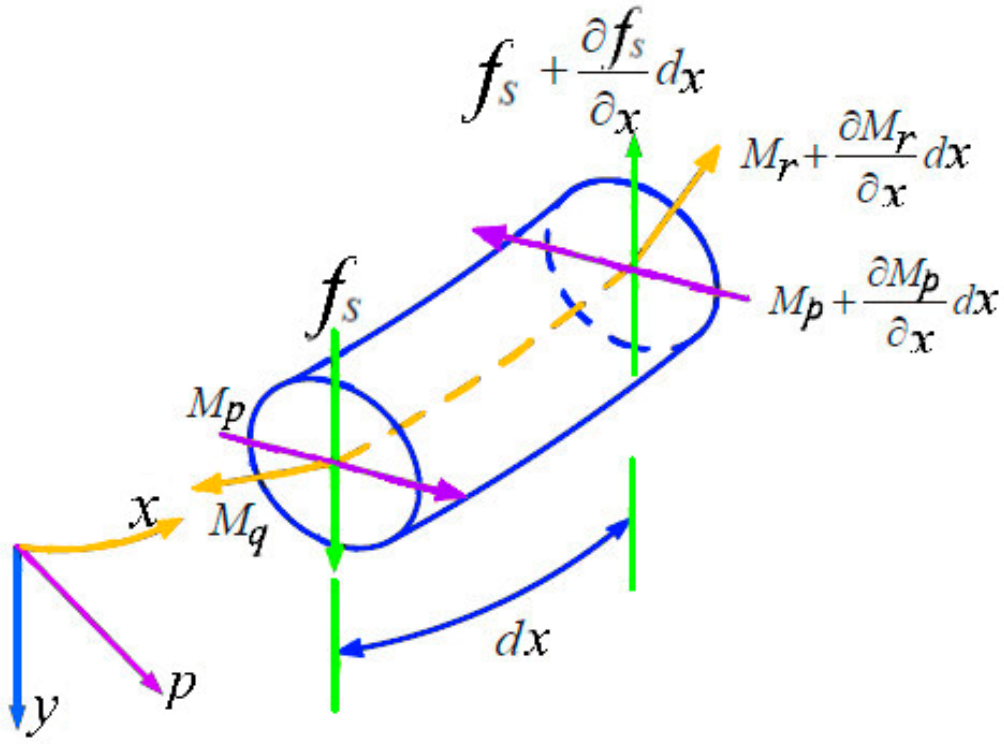


**Figure 18.** Curved beam diagram: coordinate definition of bending stiffness and shear force.

## 5. Conclusions

This paper briefly reviews the theoretical model developments on the dynamics of net cages and the hydroelastic response of floating elastic floaters of a single and array of net cages under non-moored, moored, and various effects on environmental conditions. The brief results, analyses, and limitations of the models developed in the literature are reviewed and discussed. The conclusions and future directions of research are summarized below:

- It was observed that a little study on the behavior of floating/submerged flexible cages via hydrodynamic analysis and hydroelasticity was found based on the analytical approach. However, considering design parameters for analysis, there is a lot to be developed.
- The mathematical formulations of the floating flexible circular fish cages with elastic floaters with mooring lines under the influence of waves and currents for the n-modes of oscillations in three dimensions are still unexplored. Further, a significant focus on the hydroelastic analysis of the elastic floaters coupled with net cages could be a major study.
- The qualitative analysis of the hydroelastic behavior of elastic floaters coupled with the dynamics of flexible net cages other than the cylindrical shape in currents with different mooring systems and the validation versus various methodologies in 3D remain unexplored.
- The mathematical model and semi-analytical solution of submerged spherical fish cages can be formulated based on flexible net cages with frame systems under different mooring systems to investigate the hydrodynamics response of the frame system and dynamics of fish nets.
- The mathematical formulation associated with fish cages combined with elastic floaters can be developed by considering both following and opposing wave-current conditions to analyze the wave-blocking phenomena in the case of an array of floating cages.
- Future studies of floating/submerged fish cage models with different mooring systems may include introducing several elastic floaters with array/multi-cage systems for different geometries and loads on the fish cages via hydroelastic parameters.
- The constraints of the analytical approach are that the suitable BCs must be linear, of a higher order of third or fifth, and satisfy the structural boundaries; hence, the solution must be a series of solutions. This current effort aims to serve as a valuable resource for future application studies, providing researchers in the field of Marine Engineering with insights into issues related to floating flexible porous net structures and hydroelastic floaters for modelling of fish cage applications to offshore aquaculture.

**Author Contributions:** Conceptualization, S.C.M. and C.G.S.; Methodology, S.C.M.; writing-original manuscript, S.C.M. and C.G.S. All authors have read and agreed to the published version of the manuscript.

**Funding:** The first author has been contracted as a Researcher by the Portuguese Foundation for Science and Technology (Fundação para a Ciência e Tecnologia-FCT), through Scientific Employment Stimulus, Individual Support under the Contract No. CEECIND/04879/2017. This work contributes to the Strategic Research Plan of the Centre for Marine Technology and Ocean Engineering (CENTEC), which is financed by FCT under contract UIDB/UIDP/00134/2020.

**Institutional Review Board Statement:** Not applicable.

**Informed Consent Statement:** Not Applicable.

**Data Availability Statement:** No new data were created or analyzed in this study. Data sharing is not applicable to this article.

**Conflicts of Interest:** The authors declare no conflicts of interest.

## Abbreviations

| | |
|---|---|
| ANSYS | Analysis System |
| BVP | Boundary Value Problem |
| BEM | Boundary Element Method |
| FEM | Finite Element Method |
| BC | Boundary Condition |
| FWD | Finite Water Depth |
| LSAM | Least Square Approximation Method |
| MEFEM | Matched Eigenfunction Expansion Method |
| MPEM | Multipole Expansion Method |
| GFT | Green's Function Technique |
| FBEM | Fourier Bessel Expansion Method |
| FPM | Flexible Porous Membrane |
| SIMA | Sequential IMage Analysis |
| WAMIT | WaveAnalysisMIT |
| 2D | Two-Dimensions |
| 3D | Three-Dimensions |
| VP | Velocity Potential |

## References


1. Klebert, P.; Su, B. Turbulence and flow field alterations inside a fish sea cage and its wake. *Appl. Ocean Res.* **2020**, *98*, 102113. [CrossRef]
2. Poizot, E.; Méar, Y.; Guillou, Y.; Bibeau, E. High resolution characteristics of turbulence tied of a fish farm structure in a tidal environment. *Appl. Ocean Res.* **2021**, *108*, 102541. [CrossRef]
3. Xu, L.; Li, P.; Qin, H.; Xu, Z. Numerical studies on wake and turbulence characteristics of aquaculture nets. *Front. Mar. Sci.* **2022**, *9*, 1055873. [CrossRef]
4. Guo, Y.C.; Mohapatra, S.C.; Guedes Soares, C. Review of developments in porous membranes and net type structures for breakwaters and fish cages. *Ocean Eng.* **2020**, *200*, 107027. [CrossRef]
5. Ma, M.; Zhang, H.; Jeng, D.S.; Wang, C.M. A Semi-Analytical Model for Studying Hydroelastic Behaviour of a Cylindrical Net Cage under Wave Action. *J. Mar. Sci. Eng.* **2021**, *9*, 1445. [CrossRef]
6. Gharechae, A.; Ketabdari, M.J.; Kitazawa, D.; Li, Q. Semi-analytical and experimental study on array of elastic circular floaters vertical motions in regular sea waves. *Ocean. Eng.* **2020**, *217*, 107851. [CrossRef]
7. Xu, Z.; Qin, H. Fluid-structure interactions of cage-based aquaculture: From structures to organisms. *Ocean Eng.* **2020**, *217*, 107961. [CrossRef]
8. Gharechae, A.; Ketabdari, M.J. Semi-analytical study on regular sea wave interaction with circular elastic floaters of aquaculture fish cages. *Aquacul. Eng.* **2020**, *91*, 102125. [CrossRef]
9. Chu, Y.I.; Wang, C.M.; Park, J.C.; Lader, P.F. Review of Cage and Containment Tank Designs for Offshore Fish Farming. *Aquaculture* **2020**, *519*, 734928. [CrossRef]
10. Fan, Z.Q.; Liang, Y.H.; Peng, Z.Y. Review of the research on the hydrodynamics of fishing cage nets. *Ocean Eng.* **2023**, *276*, 114192. [CrossRef]
11. Klebert, P.; Lader, P.; Gansel, L.; Oppedal, F. Hydrodynamic interactions on net panel and aquaculture fish cages: A review. *Ocean Eng.* **2023**, *58*, 260–274. [CrossRef]
12. Edwards, P. Aquaculture environment interactions: Past, present, and likely future trends. *Aquaculture* **2015**, *447*, 2–14. [CrossRef]
13. Morro, B.; Davidson, K.; Adams, T.P.; Falconer, L.; Holloway, M.; Dale, A.; Aleynik, D.; Thies, P.R.; Khalid, F.; Hardwick, J.; et al. Offshore aquaculture of finfish: Big expectations at sea. *Aquaculture* **2022**, *14*, 791–815. [CrossRef]
14. Chu, Y.I.; Wang, C.M.; Zhang, H.; Abdussamie, N.; Karampour, H.; Jeng, D.S.; Baumeister, J.; Aland, P.A. Offshore Fish Farms: A Review of Standards and Guidelines for Design and Analysis. *J. Mar. Sci. Eng.* **2023**, *11*, 762. [CrossRef]
15. Mohapatra, S.C.; Bernardo, T.A.; Guedes Soares, C. Dynamic wave induced loads on a moored flexible cylindrical net cage with analytical and numerical model simulations. *Appl. Ocean. Res.* **2021**, *110*, 102591. [CrossRef]
16. Losada, I.J.; Losada, M.A.; Martin, F.L. Experimental study of wave induced flow in a porous structure. *Coast. Eng.* **1995**, *27*, 77–98. [CrossRef]
17. Ma, M.; Zhang, H.; Jeng, D.S.; Wang, C.M. Analytical solutions of hydroelastic interactions between waves and submerged open-net fish cage modeled as a porous cylindrical thin shell. *Phy. Fluids* **2022**, *34*, 017104. [CrossRef]
18. Chwang, A.T.; Chan, A.T. Interaction between porous media and wave motion. *Annu. Rev. Fluid. Mech.* **1998**, *30*, 53–84. [CrossRef]
19. Strand, I.M.; Faltinsen, O.M. Linear sloshing in a 2D rectangular tank with a flexible sidewall. *J. Fluids Struct.* **2017**, *73*, 70–81. [CrossRef]
20. Chan, A.T.; Lee, S.W.C. Wave characteristics past a flexible fishnet. *Ocean Eng.* **2001**, *28*, 1517–1529. [CrossRef]

21. Li, B.; Liu, Z.; Liang, H.; Zheng, M.; Qiao, D. BEM modeling for the hydrodynamic analysis of the perforated fish farming vessel. *Ocean Eng.* **2023**, *285*, 115225. [CrossRef]
22. Lyu, Z.; Liu, Y.; Li, H.; Mori, N. Iterative multipole solution for wave interaction with submerged partially perforated semi-circular breakwater. *Appl. Ocean Res.* **2020**, *97*, 102103. [CrossRef]
23. Mohapatra, S.C.; Guedes Soares, C. Hydroelastic Response to Oblique Wave Incidence on the Floating Plate with a Submerged Perforated Base. *J. Mar. Sci. Eng.* **2022**, *10*, 1205. [CrossRef]
24. Cho, I.H.; Kim, M.H. Transmission of oblique incident waves by a submerged horizontal porous plate. *Ocean Eng.* **2013**, *61*, 56–65. [CrossRef]
25. Madsen, O.S. Wave transmission through porous structures. *J. Waterw. Harb. Coast. Eng. Div.* **1974**, *100*, 169–188. [CrossRef]
26. Chwang, A.T. A porous-wavemaker theory. *J. Fluid. Mech.* **1983**, *132*, 395–406. [CrossRef]
27. Molin, B. Hydrodynamic modelling of perforated structures. *Appl. Ocean Res.* **2011**, *33*, 1–11. [CrossRef]
28. Molin, B.; Remy, F. Experimental and numerical study of the sloshing motion in a rectangular tank with a perforated screen. *J. Fluids Struct.* **2013**, *43*, 463–480. [CrossRef]
29. Liu, Z.; Mohapatra, S.C.; Guedes Soares, C. Finite Element Analysis of the Effect of Currents on the Dynamics of a Moored Flexible Cylindrical Net Cage. *J. Mar. Sci. Eng.* **2021**, *9*, 159. [CrossRef]
30. Mohapatra, S.C.; Guedes Soares, C. Effect of submerged horizontal flexible membrane on moored floating elastic plate. In *Maritime Technology and Engineering*; Soares, G., Santos, Eds.; Taylor & Francis Group: London, UK, 2016; Volume 3, pp. 1181–1188.
31. Mohapatra, S.C.; Guedes Soares, C. 3D hydroelastic modelling of fluid-structure interactions of porous flexible structures. *J. Fluids Struct.* **2022**, *112*, 103588. [CrossRef]
32. Mandal, S.; Datta, N.; Sahoo, T. Hydroelastic analysis of surface wave interaction with concentric porous and flexible cylinder systems. *J. Fluids Struct.* **2013**, *42*, 437–455. [CrossRef]
33. Strand, I.M.; Faltinsen, O.M. Linear wave response of a 2D closed flexible fish cage. *J. Fluids Struct.* **2019**, *87*, 58–83. [CrossRef]
34. Su, W.; Zhan, J.M.; Huang, H. Wave interactions with a porous and flexible cylindrical fish cage. *Procedia Eng.* **2015**, *126*, 254–259. [CrossRef]
35. Mandal, S.; Sahoo, T. Gravity wave interaction with a flexible circular cage system. *Appl. Ocean Res.* **2016**, *58*, 37–48. [CrossRef]
36. Zhao, F.; Bao, W.; Kinoshita, T.; Itakura, H. Theoretical and Experimental Study on a Porous Cylinder Floating in Waves. *J. Offshore Mech. Arct. Eng.* **2010**, *133*, 011301. [CrossRef]
37. Ito, S.; Kinoshia, T.; Bao, W. Hydrodynamic behaviors of an elastic net structure. *Ocean Eng.* **2014**, *92*, 188–197. [CrossRef]
38. Ma, M.; Zhang, H.; Jeng, D.S.; Wang, C.M. Hydroelastic interactions between waves and an array of submersible flexible fish cages. *Ocean Eng.* **2022**, *266*, 113035. [CrossRef]
39. Abul-Azm, A.; Williams, A. Interference effects between flexible cylinders in waves. *Ocean Eng.* **1987**, *14*, 19–38. [CrossRef]
40. Park, M.-S.; Koo, W.-C.; Choi, Y.-R. Hydrodynamic interaction with an array of porous circular cylinders. *Int. J. Nav. Arch. Ocean Eng.* **2010**, *2*, 146–154. [CrossRef]
41. Mohapatra, S.C.; Guedes Soares, C. A semi-analytical model of an array of moored floating flexible offshore net cages under current loads. *Ocean Eng.* **2024**, *291*, 116309. [CrossRef]
42. Liu, J.; Guo, A.; Li, H. Analytical solution for the linear wave diffraction by a uniform vertical cylinder with an arbitrary smooth cross-section. *Ocean Eng.* **2016**, *126*, 163–175. [CrossRef]
43. Zheng, S.; Zhang, Y.; Liu, Y.; Iglesias, G. Wave radiation from multiple cylinders of arbitrary cross sections. *Ocean Eng.* **2020**, *184*, 11–22. [CrossRef]
44. Zhan, J.M.; Jia, X.P.; Li, Y.S.; Sun, M.G.; Guo, G.X.; Hu, Y.Z. Analytical and experimental investigation of drag on nets of fish cages. *Aqua. Eng.* **2006**, *35*, 91–101. [CrossRef]
45. Gharechae, A.; Ketabdari, M.J. Semi-analytical study of wave interaction with a submerged permeable sphere applied on a spherical aquaculture cage. *Ocean Eng.* **2023**, *272*, 113839. [CrossRef]
46. Bishop, R.E.D.; Price, W.G. *Hydroelasticity of Ships*; Cambridge University Press: Cambridge, UK, 1979.
47. Dong, G.H.; Hao, S.H.; Zhao, Y.P.; Zong, Z.; Gui, F.K. Elastic responses of a flotation ring in water waves. *J. Fluids Struct.* **2010**, *26*, 176–192. [CrossRef]
48. Li, L.; Fu, S.X.; Xu, Y.W.; Wang, J.G.; Yang, J.M. Dynamic responses of fish cage in waves and current. *Ocean Eng.* **2013**, *72*, 297–303. [CrossRef]
49. Li, P.; Faltinsen, O.M. Wave induced response of an elastic circular collar of a floating fish farm. In Proceedings of the 10th International Conference on Hydrodynamics (ICHD 2012), St. Petersburg, Russia, 1–4 October 2012; Volume 2, pp. 58–64.
50. Bardestani, M.; Faltinsen, O.M. A two-dimensional approximation of a floating fish farm in waves and current with the effect of snap loads. In Proceedings of the International Conference on Offshore Mechanics and Arctic Engineering. American Society of Mechanical Engineers, Nantes, France, 9–14 June 2013; Volume 9.
51. Shen, Y.G.; Greco, M.; Faltinsen, O.M. Numerical study of a coupled well boat-fish farm system in waves and current during loading operations. *J. Fluids Struct.* **2016**, *84*, 77–96. [CrossRef]